Nanostructured Metallic Thin Films: Measurement of Critical Exponents

L.L. Melo, R.J.C. Farias, M.C. Salvadori, M. Cattani

Instituto de Física, Universidade de São Paulo, C.P.66318, CEP 05315-970, São Paulo, SP, Brazil, mcattani@if.usp.br

Abstract

We have fabricated gold and platinum thin films by metal plasma ion deposition on silicon substrates The roughness of these nanostructured films have been measured by scanning tunneling microscopy (STM) and we have determined the growth dynamics critical exponents.

Keywords: Thin films, platinum, gold, critical exponents.

1. Introduction

Over the last past decade there was an explosion in both academic and industrial interest in nanostructured materials.[1-3] These materials may be defined as those materials whose structural elements-clusters, crystallites or molecules, have dimensions in the 1 to 100 nm range. This interest is due to the remarkable variations in fundamental electrical, optical, mechanical and magnetic properties. So, such materials have been developed and investigated due to both scientific and technological significance in recent years. With this in mind, we have fabricated nanostructured thin films by "Metal Plasma Immersion Ion Implantation and Deposition" (MePIIID).[4-9] In this technique the plasma is formed in a small vacuum arc plasma gun.[10] It is filtered for the removal of particles of cathode debris by passage through a 90° curved magnetic duct, and allowed to deposit on a substrate that can be repetitively pulsed-biased to a selected negative voltage. The ions of the depositing plasma stream are accelerated across the plasma sheath so formed, and the energy of the depositing ion flux can in this way be precisely controlled. Very high quality films can be fabricated, with structural control virtually down to the monolayer level.

We have recently fabricated, with the above described method, a series of platinum films and studied their growth dynamics.[4] In this work, following the same procedure,[4] we have deposited a series of gold films with seven different deposition times. We measured the roughness of these nanostructured films using a Scanning Tunneling Microscope (STM) and the gold grain sizes by X ray diffraction. Using the roughnesses, we have determined the scaling exponents, α and β, which characterize the dynamics of the film growth process.[11] We verified that, for short length scale, the diffusion process is dominant and that, for large length scale, the growth dynamics is essentially described by desorption and nonlinear effects.

Gold and platinum results are compared in the present work.

2. Materials and Methods

We have deposited a series of gold thin films, using "Metal Plasma Immersion Ion Implantation and Deposition" (MePIIID) on monocrystalline silicon substrates. The incident gold ion energy was about 49 eV.[12] The gold plasma was formed in a repetitively pulsed mode with 5 ms pulses at a rate of 1 pulse/sec; so the duty cycle of the deposition process was thus 0.5%. The gold cathode purity was 99.99%. Seven different gold thin film samples were made, using 200, 325, 540, 685, 870, 1140 and 1440 pulses for the depositions. Since the plasma deposition duty cycle was 0.5%, these samples correspond to film growth times t = 1.0, 1.6, 2.7, 3.4, 4.3, 5.7 and 7.2 s, respectively.

The seven gold films were analyzed with a Scanning Tunneling Microscope (STM), a NanoScope IIIA from Digital, using tungsten tips that we have fabricated. The thicknesses of the films were determined using AFM, following the same technique adopted in our preceding paper.[4]

The crystallographic grain sizes were measured by X ray diffraction, for each gold film thickness.

3. Results

All STM images are of size (1000 x 1000) nm^2 and have been obtained with a pixel size of 2 nm. In the analysis of the images, we used the zoom facility of the microscope where the maximum zoom used was (20 x 20) nm^2; thus the minimum number of pixels in the zoomed images was around 100. Figure 1 shows typical STM micrographs (1000 x 1000) nm^2 of the gold films, for the deposition t = 7.2s. Note that the scales, in

the z direction, is 20 nm/division and, in the x and y directions, are 200 nm/division. So, the images are expanded in the z direction, emphasizing the grains profile.

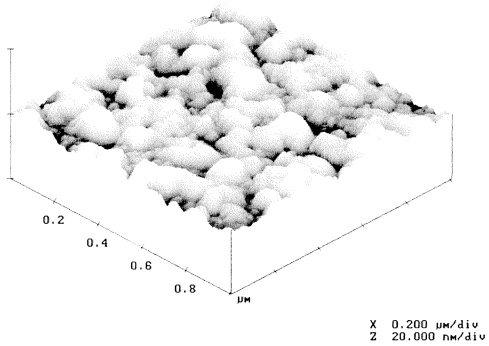

Figure 1: Typical STM micrograph of the gold film for the deposition time t = 7.2s.

The image reveals a surface formed of grains separated by voids, very similar to those observed, for instance, in gold vapor depositions on glass substrates.[13, 14] The heights and the widths of the grains increase with the deposition time t. Measuring the morphological grains size S, for t = 7.2s, we found an average value $\langle S(7.2s) \rangle \approx 110$ nm. Concerning to the thickness T(t) of the gold films as a function of the deposition time t, we found that T(t) = a t, where a = (28 ± 1) nm/s.

We have also measured the crystallographic grain sizes S by X ray diffraction for each gold film thickness. The grain size saturates for T ≥ 98 nm. For 98 ≥ T ≥ 38 nm , <S> is given by $< S > \approx 2.82\ T^{0.61}$. The morphological grains (see, for instance, Figure 1) are, actually, an agglomerated of crystallographic grains, with a cauliflower structure.

To determine the exponents, α and β, we followed the same procedure adopted in previous works.[4, 15-19] We measured the roughness in several different sites on each of the seven samples, each of area 1000 x 1000 nm^2. To obtain α, we have taken into account only the roughness of the longest deposition time film that, in the present case, is equal to t =7.2 s. This was done because the α power law becomes more clearly defined [4, 15-19] for high deposition times. With the zoom facility of the STM, we divided the (1000 x 1000) nm^2 regions into smaller regions ("windows") of size (ℓ x ℓ) nm^2, with ℓ varied from 20 to 1000 nm, and measured the local roughness $\omega(\ell,t)$.

Figure 2 shows a log-log plot of $\log_{10}\omega(\ell, t = 7.2s)$ as a function of $\log_{10}(\ell)$ where $\log_{10}\omega(\ell, t = 7.2s)$ is an average value obtained from 15 different sites on the sample. Figure 2 indicates that there are two different scaling regions: a small length scaling region R_1, for 20 nm ≤ ℓ ≤ 80 nm, and a large length scaling region R_2 , for 140 nm < ℓ ≤ 324 nm. These regions are separated by a characteristic length scale $\ell_x \approx 110$ nm. For 430 nm ≤ ℓ ≤ 570 nm we have a transition region where $\omega(\ell, t)$ begins to converge to a constant maximum local roughness value $\omega_{max}(t) = W(t)$, according to the Family-Vicsek relations.[11, 20] That is, $\omega(\ell, t) \approx$ constant = W (t) for $\ell \geq \xi$, where ξ is the "correlation length". From Figure 2 we obtain that $\xi(7.2s) \approx 500$ nm.

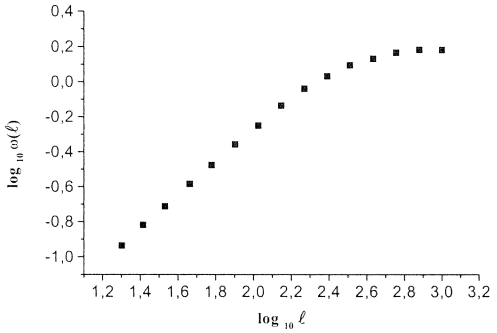

Figure 2: Plot of $\log_{10}\omega(\ell , t = 7.2 s)$ x $\log_{10}(\ell)$, where $\log_{10}\omega(\ell , t = 7.2 s)$ is an average value obtained from several sites on the sample.

The critical exponents α have been determined by using a straight-line best fit. For the first region (R_1) we obtain $\alpha_1 = 0.96 \pm 0.01$ and for the second region (R_2), $\alpha_2 = 0.63 \pm 0.04$. As the grain size is $\langle S \rangle \approx 110$ nm, in region R_1 we measured a roughness of gold surface covering, on average, only one grain or only one valley. In region R_2 the roughness is for regions covering at least two grains and the valleys between them. Since $\alpha_1 \neq \alpha_2$, the growth regimes for these two regions are different, in agreement with recent experimental results for metal thin films.[4,11,13,14,21,22] Our α_1 value is in good agreement with the value $\alpha = 0.96 \pm 0.03$ found by Krim et al.[21] for gold films for the small length scale $\ell \leq 80$ nm.

According to the Family-Vicsek approach,[15-20] to determine the growth exponent β we must take into account the W(t) values.

In Figure 3 we see $\log_{10}W(t)$ as a function of $\log_{10}(t)$, where t is the deposition time and W(t) is given by the average values of the roughness of the (1000 x 1000) nm^2 windows of several different regions for each sample. The β exponent was determined considering all W(t) values, following Family-Vicsek.[4,15-20] With a straight-line best fit, we found $\beta_2 = 0.43 \pm 0.07$, where the subscript 2 corresponds to the large-scale region, as for α_2. We verified that W(t), as a function of T, obeys the equation, $W \approx C\, T^{\beta 2}$, where C = 0.56.

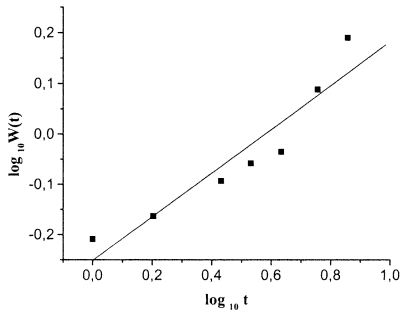

Figure 3: Plot of $\log_{10}W(t)$ x $\log_{10}(t)$ using values given in Table 3.

Now defining $z = \alpha/\beta$ and putting $\alpha_2 = 0.63 \pm 0.04$ and $\beta_2 = 0.43 \pm 0.07$, we verify that $\alpha + z = 2.09 \pm 0.19$.

In next section, taking into account our experimental values for α and β, we determine the growth dynamics of the plasma-deposited Au films and compare with the platinum films.

4. Discussions and Conclusions

Many numerical discrete models and stochastic partial differential equations have been proposed[11,23-25] to explain the growth of metallic thin films produced by ion deposition and vapor deposition. It is not our intention here to consider and analyze the most general and complete stochastic equations found in the literature.[11,23,24] As pointed out in our recent paper,[4] we believe that the following equation contains all the physically relevant growth mechanisms for metallic films:[11,24]

$$\partial h/\partial t = \nu\nabla^2 h+(\lambda/2)(\nabla h)^2-K\nabla^4 h+F(\mathbf{x},t)+\eta(\mathbf{x},t), \quad (1)$$

where $h(\mathbf{x},t)$ is the surface height, the first two terms, proportional to ν and λ, represent the desorption and nonlinear effects, respectively, the term with K is responsible for the surface diffusion, $F(\mathbf{x},t)$ is the incoming atomic flux and, finally, $\eta(\mathbf{x},t)$ is a noise function reflecting random deposition effects. The flux term $F(\mathbf{x},t)$ will be omitted in what follows because it does not affect the scaling exponents. As is well known,[4,11,23,24] the competition between the desorption and diffusion terms in Eq. (1) generates a characteristic length scale ℓ_x. By scaling arguments it can be shown that for short length scale ($\ell < \ell_x$) the diffusive term determines the scaling behavior, while for large length scale ($\ell > \ell_x$) the desorption term governs the scaling.[4,11,23,24] Indeed, since in region R_1, $\alpha_1 = 0.96 \pm 0.01$, that is $\alpha \approx 1$, it seems that for this region the growth equation is given by:[11]

$$\partial h/\partial t = -K\nabla^4 h + \eta_1(\mathbf{x},t) \quad , \quad (2)$$

where $\eta_1(\mathbf{x},t)$ is a Gaussian noise function. As seen elsewhere,[11] Eq. (2) predicts $\alpha = 1$ for a bidimensional surface. This implies that the dynamics is dominated by surface diffusion during the grain growth, as nicely illustrated by the experiments of Tong et al.[26,27] for Au films, and by our experiments for Pt films.[4]

On the other hand, for large length scale, that is for $\ell > \ell_x \approx 110$ nm, the desorption and nonlinear terms are expected to be dominant.[4,11,17,18] For these conditions, putting $K \approx 0$ in Eq. (1) we would have an equation, known as the Kardar-Parisi-Zhang equation, or simply the KPZ equation:

$$\partial h/\partial t = \nu\nabla^2 h + (\lambda/2)(\nabla h)^2 + \eta_2(\mathbf{x},t) \, . \quad (3)$$

For large length scale and for deposition times sufficiently long, the KPZ equation is expected[11,24] to describe the final roughness and dynamics, no matter how important is the diffusion process. Indeed, according to Section 3, $\alpha_2 = 0.63 \pm 0.04$, $\beta_2 = 0.43 \pm 0.07$ and consequently $\alpha + z = 2.09 \pm 0.19$. That is, the "KPZ signature", that is $\alpha + z = 2$, is obeyed within the experimental errors. This is evidence for the validity of the KPZ equation. On the other hand, numerical simulations of the KPZ equation, for d = 2 ballistic deposition and with a Gaussian noise function,[28] give $\alpha = 0.38$ and $\beta = 0.24$. These predicted exponents are very different from $\alpha_2 \approx 0.63$ and $\beta_2 \approx 0.4$ obtained in this paper.

These discrepancies can be explained as due to long range spatial and temporal correlations in the noise function $\eta_2(\mathbf{x},t)$, as occurs with the platinum films[4]. In the present gold case, we have found the exponents characterizing the decay of spatial and temporal correlations, ψ and θ, respectively , given by $\psi = 0.6$ and $\theta = 0.25$. Since $\psi < 1$ and $\theta < ½$, they obey, according to Medina et al.,[29] necessary conditions to have a meaningful

correlation noise effects within the KPZ approach. Thus, our analysis shows that it is plausible that the growth mechanism, for large-scale lengths $\ell > 106$ nm, is governed by the KPZ equation. This was also verified for platinum films for $\ell > 25$nm.[4]

Acknowledgements

This work was supported by the FAPESP (Fundação de Amparo à Pesquisa do Estado de São Paulo) and by the CNPq (Conselho Nacional de Desenvolvimento Científico e Tecnológico). The authors are grateful to the "Laboratório de Cristalografia" of the Institute of Physics of the University of São Paulo, for the X-ray analysis.

References

[1] P. Moriarty, Rep. Progr. Phys. **64**, 297 (2001)
[2] N. Cowlam, Solid State Phenom. **56**, 145 (1997)
[3] H. Gleiter, Acta Mater. **48**, 1 (2000)
[4] M.C. Salvadori, L.L. Melo, M. Cattani, O.R. Monteiro and I.G. Brown – "Measurement of critical exponents of platinum thin films". Accepted for publication in Surface Review and Letters (2003).
[5] "Handbook of Plasma Immergion Ion Implantation and Deposition". Edited by A. Anders – John Wiley & Sons, Inc.
[6] I.G. Brown, *Annual Review of Materials Science,* Vol. 28, (Annual Reviews, Inc., Palo Alto, CA, 1998).
[7] O.R. Monteiro, Nucl. Instrum. Meth. Phys. Res. **B148**, 12-16 (1999).
[8] I.G. Brown, A. Anders, M.R. Dickinson, R.A. MacGill and O.R. Monteiro, Surf. Coat. Technol. **112**, 271-277 (1999).
[9] G.M. Pharr, D.L. Callahan, S.D. McAdams, T.Y. Tsui, S. Anders, A. Anders, J.W. Ager I.G. Brown, C.S. Bhatia, S.R.P. Silva and J. Robertson, Appl. Phys. Lett. **68**, 779-781 (1996).
[10] R.A. MacGill, M.R. Dickinson, A. Anders, O.R. Monteiro and I.G. Brown, Rev. Sci. Instrum. **69**, 801-803 (1998).
[11] A.L. Barabasi and H.E. Stanley, *Fractal Concepts in Surface Growth* (Cambridge University Press, 1995).
[12] A. Anders and G. Yu. Yushkov , J. Appl. Phys. (2002),accepted for publication.
[13] P. Herrasti, P. Ocón, L. Vásquez, R. C. Salvarezza, J. M. Vara and A. J. Arvia, Phys. Rev **A45**, 7440-7446 (1992).
[14] R.C. Salvarezza, L. Vásquez, P. Herrasti, P. Ocón, J.M. Vara and A.J. Arvia, Europhys. Lett. **20**, 727-732 (1992).
[15] M.C. Salvadori, M.G. Silveira and M. Cattani, Phys. Rev. **E58**, 6814-6816 (1998).
[16] M.C. Salvadori, M.G. Silveira and M. Cattani, Thin Solid Films **376**, 264-266 (2000).
[17] M.C. Salvadori, A.M. Pizzo and M. Cattani, Surf. Rev. Lett. **8**, 291-294 (2001).
[18] M. Cattani, and M.C. Salvadori, Surf. Rev. Lett. **8**, 347-341 (2001).
[19] M.C. Salvadori, L.L. Melo, D.R. Martins, A.R. Vaz and M. Cattani, Surf. Rev. Lett. (2002), accepted for publication.
[20] F. Family and T. Vicsek, J. Phys. **A18**, L75-L81 (1985).
[21] J. Krim, I. Heyvaert, C. Van Haesendock and Y. Bruynseraede, Phys. Rev. Lett. **70**, 57-60 (1993).
[22] J.M. Gómez Rodriguez, A.M. Baró and R.C. Salvarezza, J. Vac. Sci. Technol. **B9**, 495- 499 (1991).
[23] P. Meakin, Phys. Rep. **235**, 189-289 (1993).
[24] D.D. Vedensky, A. Zangwill and C.N. Luse, Phys. Rev. **E48**, 852-862 (1993).
[25] I.T. Koponen, Nucl. Instr. and Method. Phys. Res. **B171**, 314-324 (2000).
[26] W.M. Tong, E.J. Snyder, R.S. Williams, A. Yanase, Y. Segawa and M. S. Anderson, Surf. Sci. Lett. **277**, L63-69 (1994).
[27] W.M. Tong and R.S. Williams, Ann. Rev. Phys. Chem.**45**, 401-438 (1994).
[28] C. Castellano,M.Marsili and L.Pietronero.Phys.Rev.Lett.**16**, 3257 (1998).
[29] E. Medina, T. Hwa and M. Kardar, Phys. Rev.**A39**, 3053-3075 (1989).
[30] J.F. Ziegler and J.P. Biersack, see for example the web site www.SRIM.org.